SUPPLEMENTARY INFORMATION
https://doi.org/10.1038/s41593-018-0113-5

nature neuroscience

In the format provided by the authors and unedited.

TDP-43 gains function due to perturbed autoregulation in a *Tardbp* knock-in mouse model of ALS-FTD

Matthew A. White[1,2,14,17], Eosu Kim[3,4,17], Amanda Duffy[5], Robert Adalbert[6], Benjamin U. Phillips[3], Owen M. Peters[7,15], Jodie Stephenson[8,16], Sujeong Yang[6], Francesca Massenzio[1,2], Ziqiang Lin[1,2], Simon Andrews[1], Anne Segonds-Pichon[1], Jake Metterville[9], Lisa M. Saksida[3,10,11], Richard Mead[8], Richard R Ribchester[12], Youssef Barhomi[13], Thomas Serre[13], Michael P. Coleman[1,6], Justin R. Fallon[5], Timothy J. Bussey[3,10,11], Robert H. Brown Jr[9] and Jemeen Sreedharan[1,2,14]*

[1]The Babraham Institute, Cambridge, UK. [2]Maurice Wohl Clinical Neuroscience Institute, Institute of Psychiatry, Psychology and Neuroscience, King's College London, London, UK. [3]Department of Psychology and MRC/Wellcome Trust Behavioural and Clinical Neuroscience Institute, University of Cambridge, Cambridge, UK. [4]Department of Psychiatry, Institute of Behavioral Science in Medicine, Brain Korea 21 Plus Project for Medical Sciences, Yonsei University College of Medicine, Seoul, Republic of Korea. [5]Department of Neuroscience, Brown University, Providence, RI, USA. [6]John van Geest Centre for Brain Repair, University of Cambridge, Cambridge, UK. [7]The Vollum Institute, Oregon Health & Science University, Portland, OR, USA. [8]Sheffield Institute for Translational Neuroscience, University of Sheffield, Sheffield, UK. [9]Department of Neurology, UMass Medical School, Worcester, MA, USA. [10]Molecular Medicine Research Group, Robarts Research Institute & Department of Physiology and Pharmacology, Schulich School of Medicine & Dentistry, Western University, London, ON, Canada. [11]The Brain and Mind Institute, Western University, London, ON, Canada. [12]SBMS, University of Edinburgh, Edinburgh, UK. [13]Department of Cognitive, Linguistic and Psychological Sciences, Brown University, Providence, RI, USA. Present address: [14]Maurice Wohl Clinical Neuroscience Institute, Institute of Psychiatry, Psychology and Neuroscience, King's College London, London, UK. [15]School of Biosciences, Dementia Research Institute, Cardiff University, Cardiff, UK. [16]Centre for Neuroscience and Trauma, Blizard Institute, Barts and the London School of Medicine and Dentistry, Queen Mary University of London, London, UK. [17]These authors contributed equally: Matthew A. White, Eosu Kim.
*e-mail: jemeen.sreedharan@kcl.ac.uk

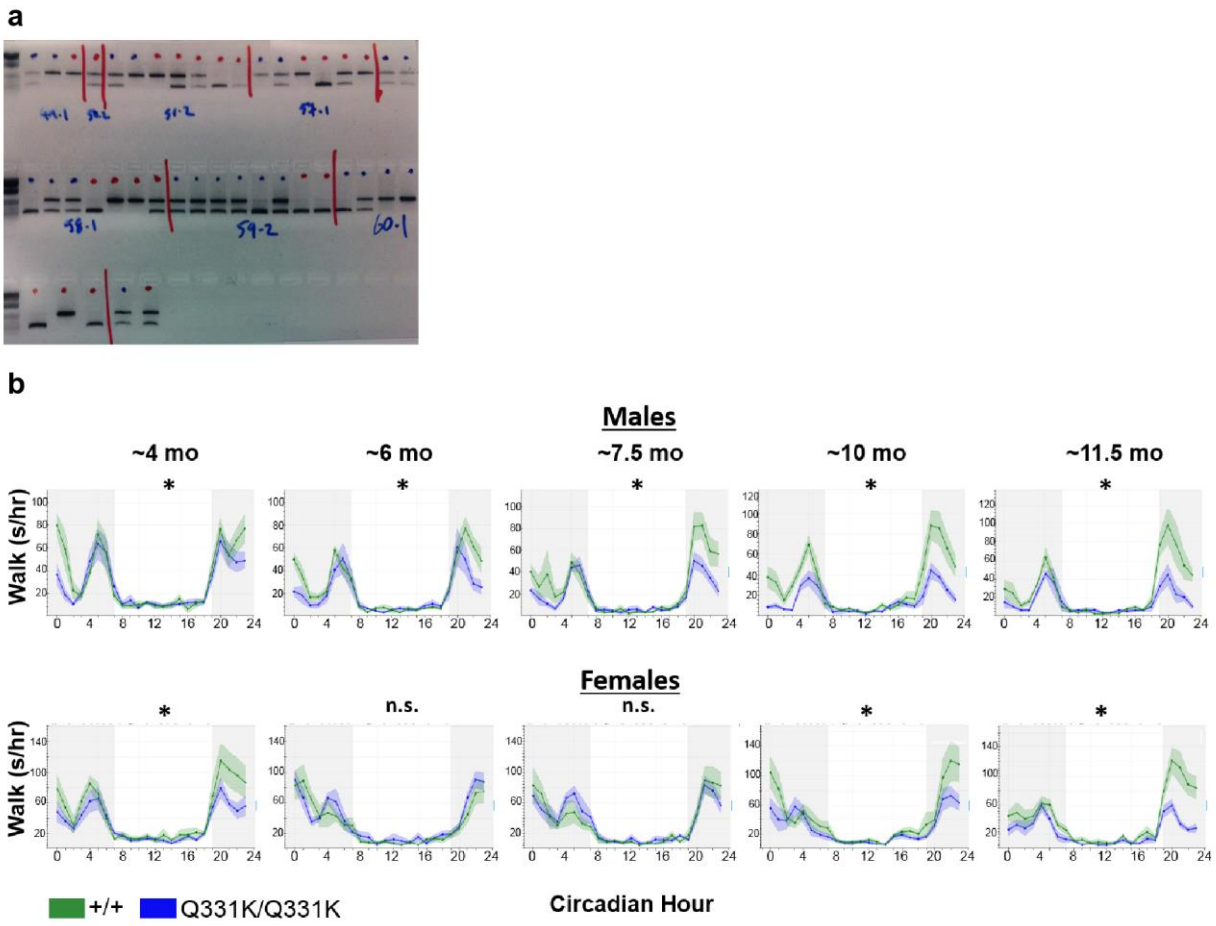

Supplementary Figure 1

ACBM walking phenotypes

(a) Uncropped agarose gel of genotyping PCR used in figure 1b.
(b) Automated continuous behavioral monitoring of walking behavior from 4 to 11.5 months of age separated by sex (n = 5 mice per genotype).
Male mice; 4 months: interaction $^{*}P=0.001$; 6 months: interaction $^{*}P=0.003$; 7.5 months: interaction $^{*}P<0.0001$;
10 months: interaction $^{*}P< 0.0001$; 11.5 months: interaction $^{*}P< 0.0001$.
Female mice; 4 months: interaction $^{*}P=0.034$; 6 months: n.s. interaction $P=0.138$; 7.5 months: n.s. interaction $P=0.334$; 10 months: interaction $^{*}P< 0.0001$; 11.5 month: interaction $^{*}P< 0.0001$; repeated measures two–way ANOVA.
Error bars represent mean ± s.e.m.

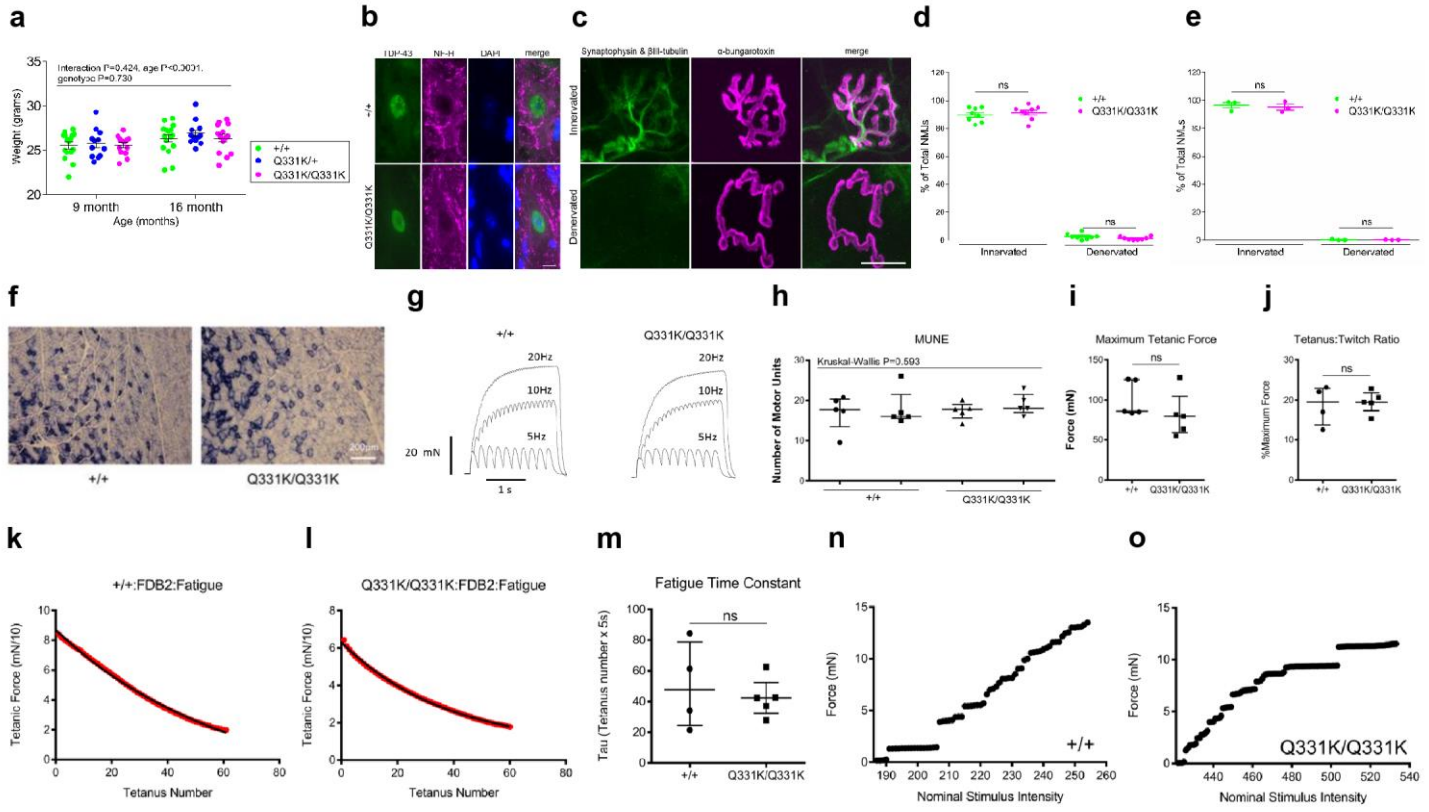

Supplementary Figure 2

Neuromuscular investigations

(a) Weights of psychology cohort 2 mice (n = 16 wild-type, 12 TDP–43$^{Q331K/+}$, 14 TDP-43$^{Q331K/Q331K}$ mice). Comparison by repeated measures two–way ANOVA.
(b) TDP–43 immunohistochemistry in motor neurons of 5–month–old mice (n = 5 mice per genotype). Representative images shown. Scale bar, 10μm.
(c) Representative examples of NMJ immunostaining in gastrocnemius muscles (scale bar, 20μm) with (d) quantification of innervation in wild–type and TDP43$^{Q331K/Q331K}$ mice at 5 months of age (n = 8 mice per genotype). Comparisons: Innervated: P=0.528 (ns); denervated: P=0.127 (ns).
(e) Innervation/denervation analysis of gastrocnemius muscles in 18 to 23–month–old wild–type and TDP43$^{Q331K/Q331K}$ mice (n = 3 mice per genotype). Comparisons: Innervated: P=0.678 (ns); denervated: P=0.801 (ns).
For (d) and (e) unpaired t test with correction using the Holm–Sidak method.
(f) Succinate dehydrogenase enzymatic activity in gastrocnemius muscles from 5–month–old mice (n = 8 mice per genotype). Representative images shown. Scale bar, 200μm.
Error bars for (a,d,e) denote s.e.m.
(g) Tetanic force responses to repetitive stimulation at 5, 10 and 20Hz from FDB-tibial nerve preparations. Representative wild–type and TDP43$^{Q331K/Q331K}$ mice are shown.
(h) Motor unit number estimates in wild–type and TDP43$^{Q331K/Q331K}$ mice based on inspection (Insp) of traces such as those shown in main Fig. 2g, and extrapolation between average motor unit size of the first four units relative to maximum muscle twitch tension (MUNE) (n = 5 wild–type and 5 TDP-43$^{Q331K/Q331K}$ mice). Comparison: Kruskal–Wallis.
(i) Maximum tetanic force in TDP43$^{Q331K/Q331K}$ mice compared with controls (50Hz stimulation) (n = 5 wild–τype and 5 TDP–43$^{Q331K/Q331K}$ mice). Comparison: P=0.150 (ns); two-tailed Mann–Whitney.
(j) Tetanus–twitch ratio (expressed as a percentage of maximum force) (n = 4 wild–type and 5 TDP–43$^{Q331K/Q331K}$ mice). Comparison: P>0.999 (ns); two-tailed Mann–Whitney.

(k,l) Fatigue profiles showing decline in maximum tetanic force with repeated stimulation (50Hz for 1 s every 5 s) in representative TDP43$^{Q331K/Q331K}$ and wild–type mouse FDB preparations.
(m) Time constant of decay of tetanic force comparing the muscles tested (n = 4 wild–type and 5 TDP–43$^{Q331K/Q331K}$ mice). Comparison: P>0.999 (ns); two-tailed Mann–Whitney.
(n,o) Contractile force measurements with progressively graded stimulation (arbitrary units) from representative wild–type and TDP–43$^{Q331K/Q331K}$ mice (n = 3 mice per genotype).
Error bars for (h,i,j,m) represent median and interquartile range.

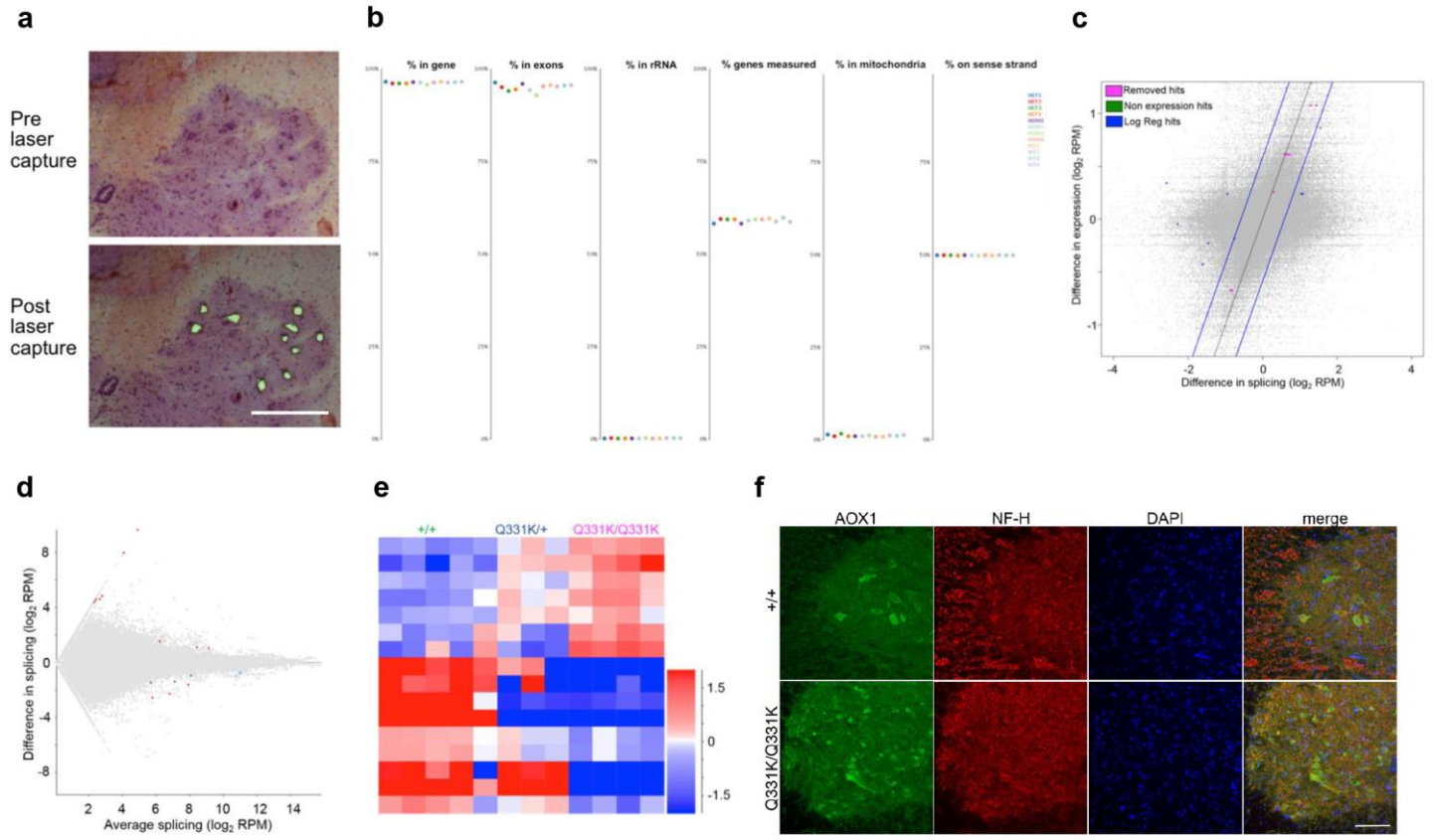

Supplementary Figure 3

Laser capture and RNA sequencing analysis of lumbar spinal motor neurons

(a) Nissl staining of lumbar spinal cord showing anterior horn motor neurons before and after laser capture (n = 4 wild-type, 4 TDP–43$^{Q331K/+}$, 4 TDP–43$^{Q331K/Q331K}$ mice). Scale bar, 300μm.
(b) Quality control measures of laser–capture RNA sequencing data. A mean of 49.9 million reads–per–mouse (range 43.7–57.3million) were obtained. Displayed is the percentage of reads that are mapped within genes and exons; reads from ribosomal or mitochondrial RNA; percentage of annotated genes measured and the percentage of reads that are mapped to the sense strand. Colored dots represent individual libraries prepared from each mouse sequenced.
(c) Filtering of lumbar spinal cord DESeq2 alternative splice events that are significantly different between wild–type and TDP–43$^{Q331K/Q331K}$ mice. Non–expression hits reflect changes in splice junction usage that exceed a 1.5–fold change relative to expression of the gene from which they are derived. Log Reg hits include splice junctions whose usage changes relative to another junction with the same start or end position.
(d) MA plot and (e) hierarchical clustering of alternative splice events in the lumbar spinal cord of wild–type and TDP–43$^{Q331K/Q331K}$ mice (n = 4 wild-type, 4 TDP–43$^{Q331K/+}$, 4 TDP–43$^{Q331K/Q331K}$ mice). Comparison: DESeq2 wild–type v TDP–43$^{Q331K/Q331K}$.
(f) Immunohistochemistry for AOX1 in lumbar motor neurons of 5–month–old mice (n = 4 wild-type, 4 TDP–43$^{Q331K/Q331K}$ mice). Representative images shown. Scale bar, 100μm.

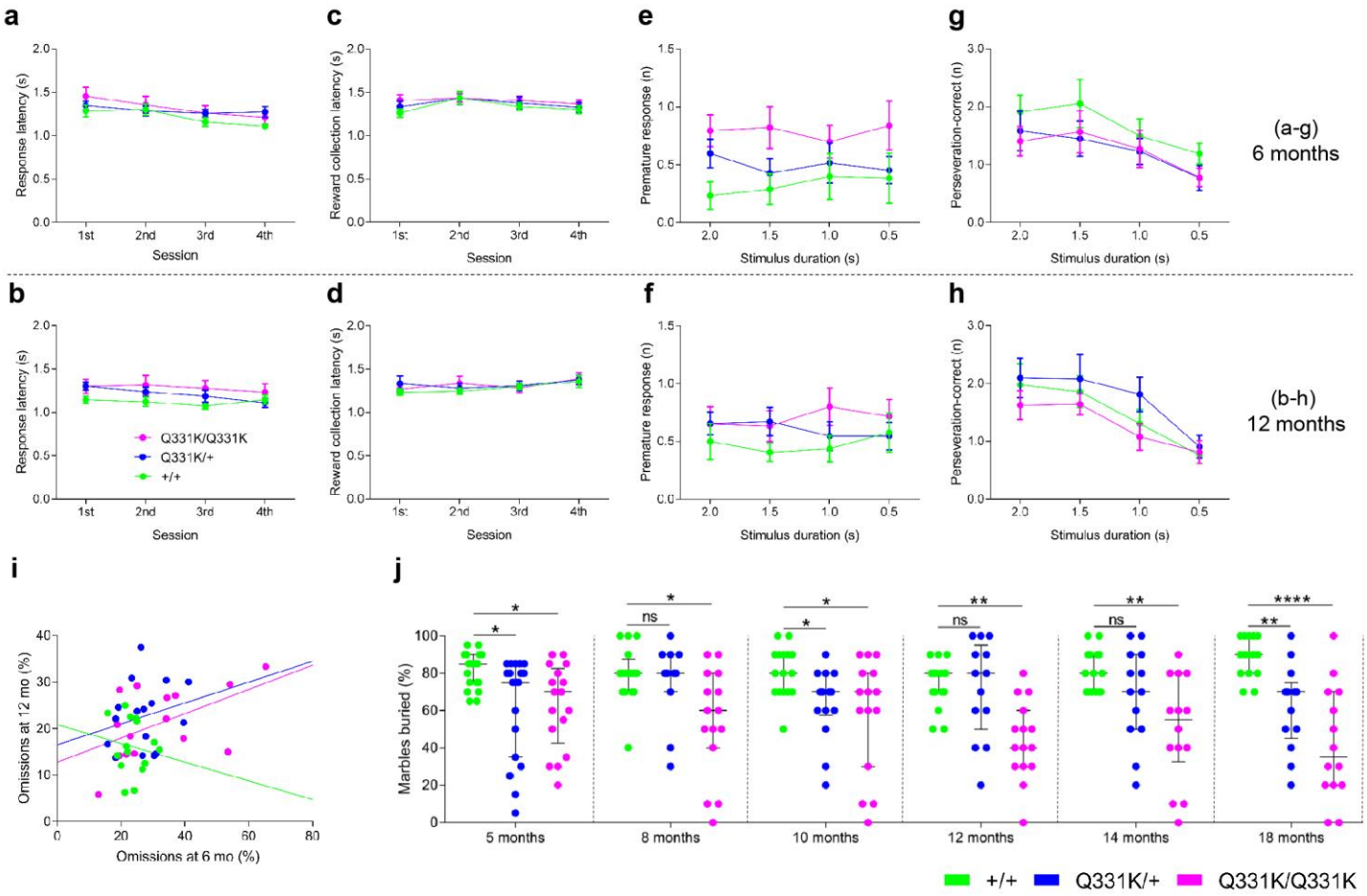

Supplementary Figure 4

Additional behavioral outcomes from five-choice serial reaction time tasks and marble burying assays

(a–b) Response latencies. Genotype comparison: P=0.448 in 6–month–old; P=0.181 12–month–old mice.
(c–d) Reward collection latencies. Genotype comparison: P=0.662 in 6–month–old; P=0.821 12–month–old mice.
(e–f) Premature responses. Genotype comparison: P=0.068 in 6–month–old; P=0.194 12–month–old mice.
(g–h) Perseverative responses after correct response. Genotype comparison: P=0.312 in 6–month–old; P=0.291 12–month–old mice. At 6 months of age, n = 15 wild–type, 16 TDP–43$^{Q331K/+}$, 15 TDP–43$^{Q331K/Q331K}$ mice, and at 12 months, n = 15 wild–type, 16 TDP–43$^{Q331K/+}$, 16 TDP–43$^{Q331K/Q331K}$ mice.
For (a–h) mixed–effects model was used and error bars denote s.e.m.
(i) Correlation between omissions at 6 and 12 months of age in individual mice (n = 15 wild–type, 16 TDP–43$^{Q331K/+}$, 15 TDP–43$^{Q331K/Q331K}$ mice). Comparisons: wild-type: P=0.600 (ns); TDP–43$^{Q331K/+}$: P=0.392 (ns); TDP–43$^{Q331K/Q331K}$: P=0.046 (∗); Pearson's analysis.
(j) Progressive marble burying of cohort 1 mice. Pairwise comparisons: 5 months (n = 19 wild–type, 19 TDP–43$^{Q331K/+}$, 17 TDP–43$^{Q331K/Q331K}$ mice); wild–type vs. TDP–43$^{Q331K/+}$: P=0.03 (∗); wild–type vs. TDP–43$^{Q331K/Q331K}$: P=0.013 (∗); 8 months (n = 16 wild–type, 11 TDP–43$^{Q331K/+}$, 15 TDP–43$^{Q331K/Q331K}$ mice); wild–type vs. TDP–43$^{Q331K/+}$: P>0.999 (ns); wild–type vs. TDP–43$^{Q331K/Q331K}$: P=0.02 (∗); 10 months (n = 16 wild–type, 14 TDP–43$^{Q331K/+}$, 15 TDP–43$^{Q331K/Q331K}$ mice); wild–type vs. TDP–43$^{Q331K/+}$: P=0.03 (∗); wild–type vs. TDP–43$^{Q331K/Q331K}$: P=0.03 (∗); 12 months (n = 16 wild–type, 13 TDP–43$^{Q331K/+}$, 15 TDP–43$^{Q331K/Q331K}$ mice); wild–type vs. TDP–43$^{Q331K/+}$: P>0.999 (ns); wild–type vs. TDP–43$^{Q331K/Q331K}$: P=0.001 (∗∗); 14 months (n = 15 wild–type, 13 TDP–43$^{Q331K/+}$, 14 TDP–43$^{Q331K/Q331K}$ mice); wild–type vs. TDP–43$^{Q331K/+}$: P=0.396 (ns); wild–type vs. TDP–43$^{Q331K/Q331K}$: P=0.003 (∗∗); 18 months (n = 15 wild–type, 13 TDP–43$^{Q331K/+}$, 14 TDP–43$^{Q331K/Q331K}$ mice); wild–type vs. TDP–43$^{Q331K/+}$: P=0.009 (∗∗); wild–type vs. TDP–43$^{Q331K/Q331K}$: P<0.0001 (∗∗∗∗); Kruskal–Wallis followed by Dunn's test for pairwise comparisons.
Error bars for (j) represent median and interquartile range.

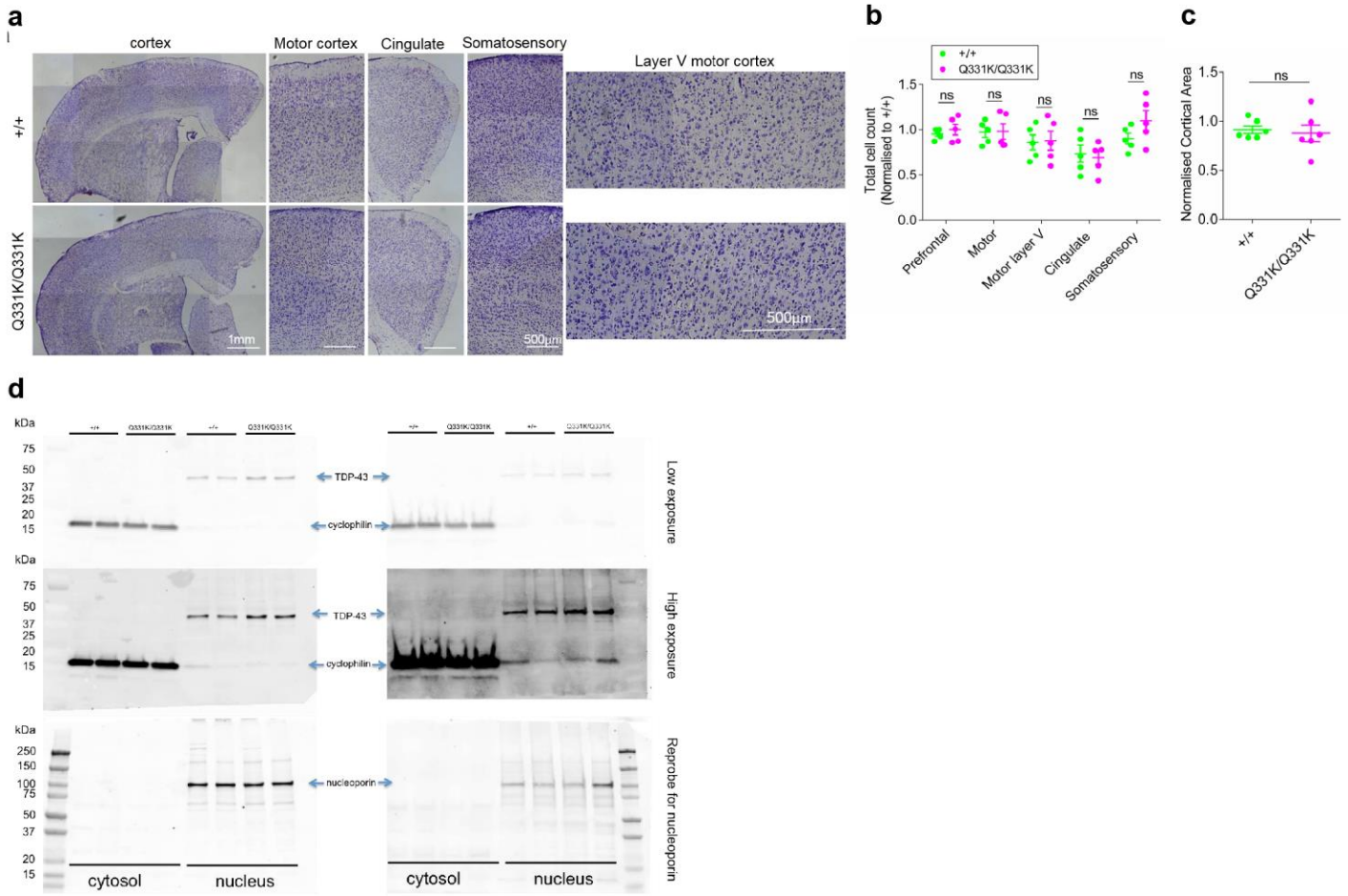

Supplementary Figure 5

Frontal cortical histology

(a) Nissl–stained coronal sections of frontal cortex. Representative images shown. Cortex scale bar, 1mm; motor, cingulate and somatosensory cortex scale bars, 500μm; motor cortex layer V scale bar, 500μm.
(b) Quantification of cells in cortical sub regions (n = 5 mice per genotype). Comparisons: Prefrontal: P=0.477(ns); Motor: P=0.931(ns); Motor layer V: P=0.897(ns); Cingulate: P=0.734(ns); Somatosensory: P=0.150(ns); multiple t tests with correction using the Holm–Sidak method.
(c) Quantification of frontal cortical area in TDP–43$^{Q331K/Q331K}$ mice relative to wild type (n = 6 mice per genotype). Comparison: P=0.701 (ns); unpaired t test.
Error bars denote s.e.m.
(d) Uncropped western blots of frontal cortical tissue from four wild–type and four TDP–43$^{Q331K/Q331K}$ mice used in the quantification of TDP–43 in figure 4e.

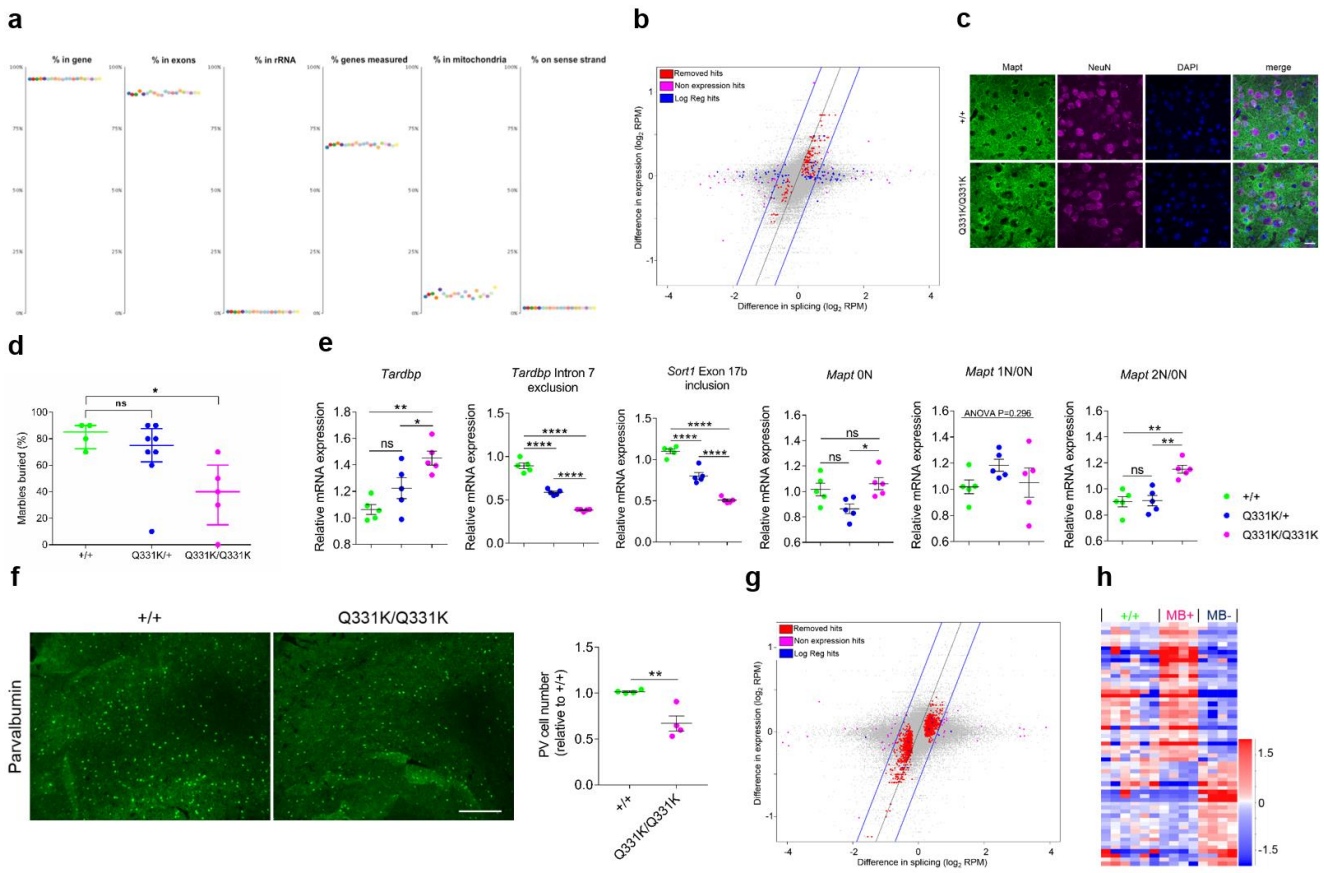

Supplementary Figure 6

Frontal cortical RNA-seq, tau staining and validation in line 3 mice

(a) Quality control measures of sequencing reads from 20 frontal cortical libraries from 5 month old mice (coloured dots represent libraries for individual mice). A mean of 58.7m reads–per–mouse (range 42.8–76.3m) were obtained.
(b) Filtering of frontal cortex DESeq2 alternative splice events that are significantly different between 5–month–old wild–type and TDP–43$^{Q331K/Q331K}$ mice. Non–expression hits reflect changes in splice junction usage exceeding a 1.5–fold change relative to expression of the gene from which they are derived. Log Reg hits include splice junctions whose usage changes relative to another junction with the same start or end position.
(c) Immunostaining for tau in the cortices of 20–month–old mice. Neuronal cells have been stained with NeuN. Representative images shown. Scale bar, 25μm.
(d) Marbles buried by line #3 mice (n = 4 wild–type, 8 TDP–43$^{Q331K/+}$, 5 TDP–43$^{Q331K/Q331K}$ mice). Pairwise comparisons: wild–type vs. TDP–43$^{Q331K/+}$: P=0.691 (ns); wild–type vs. TDP–43$^{Q331K/Q331K}$: P=0.020 (*); Kruskal–Wallis followed by Dunn's test. Error bars represent median and interquartile range.
(e) qPCR of expression and splicing changes in line #3 mice (n = 5 wild–type, 5 TDP–43$^{Q331K/+}$, 5 TDP–43$^{Q331K/Q331K}$ mice). Pairwise comparisons: *Tardbp* expression: wild–type vs. TDP–43$^{Q331K/+}$: P=0.076 (ns); wild–type vs. TDP–43$^{Q331K/Q331K}$: P=0.0016 (**); TDP–43$^{Q331K/+}$ vs. TDP–43$^{Q331K/Q331K}$: P=0.036 (*); 0N: wild–type vs. TDP–43$^{Q331K/+}$: P=0.072 (ns); wild–type vs. TDP–43$^{Q331K/Q331K}$: P=0.495 (ns); TDP–43$^{Q331K/+}$ vs. TDP–43$^{Q331K/Q331K}$: P=0.03 (*); 2N/0N: wild–type vs. TDP–43$^{Q331K/+}$: P=0.877 (ns); wild–type vs. TDP–43$^{Q331K/Q331K}$: P=0.002 (**); TDP–43$^{Q331K/+}$ vs. TDP–43$^{Q331K/Q331K}$: P=0.002 (**); P<0.0001 (****); one–way ANOVA followed by Holm–Sidak post–hoc tests for pairwise comparisons. Error bars denote s.e.m.
(f) Immunohistochemistry for parvalbumin in cortices of line #3 mice. Representative images shown. Scale bar, 250μm and quantification of parvalbumin–positive neurons (n = 4 mice per genotype). Comparison: P=0.006 (**); unpaired t test. Error bars denote s.e.m.
(g) Filtering of 5–month–old frontal cortex DESeq2 alternative splice events that are significantly different between MB+ and MB– TDP–43$^{Q331K/Q331K}$ mice. Refer to subfigure (b).
(h) Hierarchical clustering of alternative splice events in 5–month–old frontal cortices comparing MB+ and MB– TDP–43$^{Q331K/Q331K}$ mice (n = 6 wild–type, 4 MB+ TDP–43$^{Q331K/Q331K}$ and 4 MB– TDP–43$^{Q331K/Q331K}$ mice); Comparison: DESeq2 MB+ vs MB–.

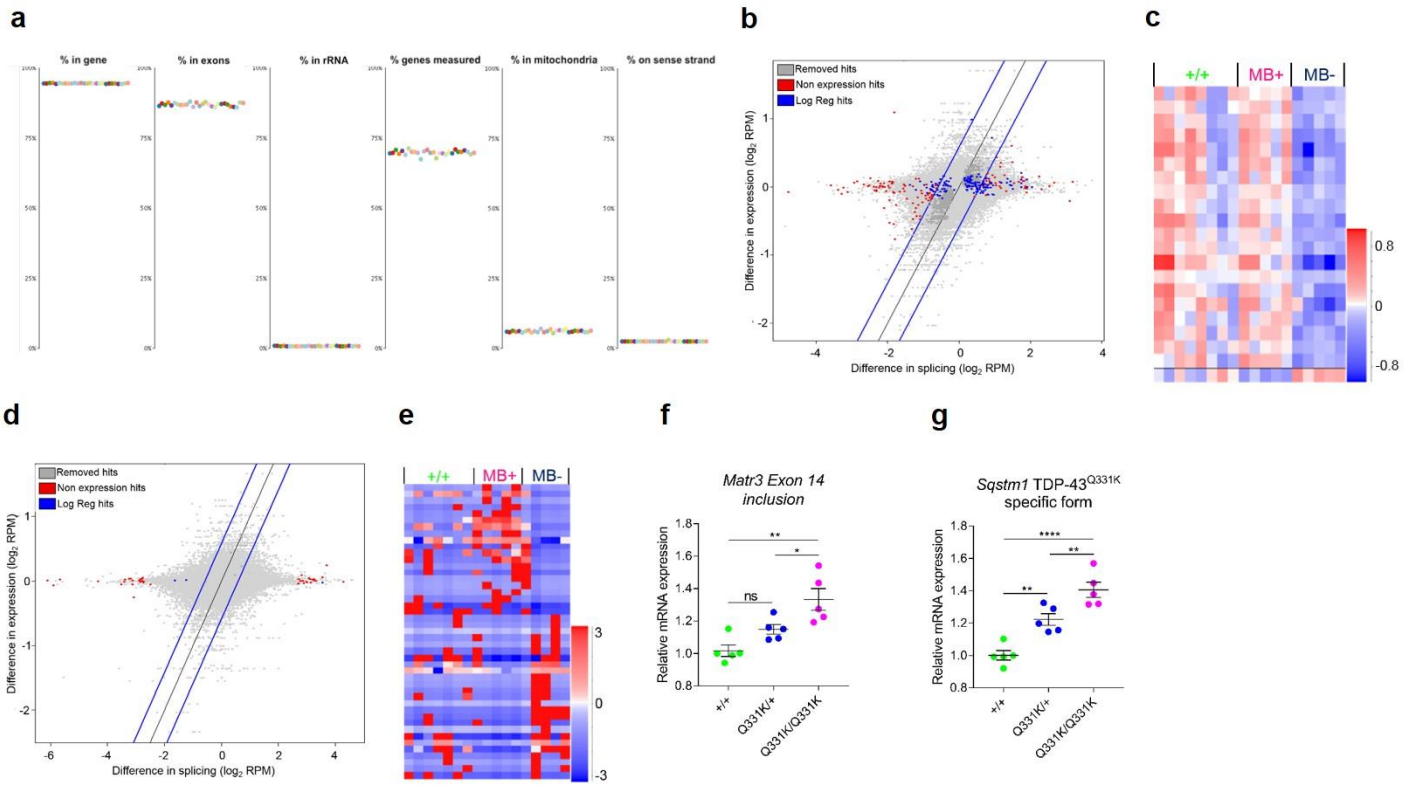

Supplementary Figure 7

RNA-seq in aged mice

(a) Quality control measures of sequencing reads from 28 frontal cortical libraries from 20–month–old mice (coloured dots represent libraries for individual mice).
(b) Filtering of 20–month–old frontal cortex DESeq2 alternative splice events that are significantly different between wild–type and TDP–43$^{Q331K/Q331K}$ mice. Non–expression hits reflect changes in splice junction usage exceeding a 1.5–fold change relative to expression of the gene from which they are derived. Log Reg hits include splice junctions whose usage changes relative to another junction with the same start or end position.
(c) Hierarchical clustering of differentially expressed genes in 20–month–old frontal cortices comparing MB+ and MB– TDP–43$^{Q331K/+}$ mice (n = 8 wild–type, 5 MB+ TDP–43$^{Q331K/+}$ and 5 MB– TDP–43$^{Q331K/+}$ mice); Comparison: DESeq2 MB+ vs MB–.
(d) Filtering of 20–month–old frontal cortex DESeq2 alternative splice events that are significantly different between MB+ and MB– TDP–43$^{Q331K/+}$ mice. Refer to subfigure (b).
(e) Hierarchical clustering of alternative splice events in 20–month–old frontal cortices comparing MB+ and MB– TDP–43$^{Q331K/+}$ mice (n = 8 wild–type, 5 MB+ TDP–43$^{Q331K/+}$ and 5 MB– TDP–43$^{Q331K/+}$ mice); Comparison: DESeq2 MB+ vs MB–.
(f) qPCR of splicing changes in *Matr3* exon 14. Pairwise comparisons: wild–type vs. TDP–43$^{Q331K/+}$: P=0.07 (ns); wild–type vs. TDP–43$^{Q331K/Q331K}$: P=0.0014 (**); TDP–43$^{Q331K/+}$ vs. TDP–43$^{Q331K/Q331K}$: P=0.033 (*).
(g) qPCR of splicing changes in *Sqstm1*. Pairwise comparisons: wild–type vs. TDP–43$^{Q331K/+}$: P=0.003 (*); wild–type vs. TDP–43$^{Q331K/Q331K}$: P<0.0001 (****); TDP–43$^{Q331K/+}$ vs. TDP–43$^{Q331K/Q331K}$: P=0.005 (**).
(f–g) For qPCR, n = 5 mice per genotype; one–way ANOVA followed by Holm–Sidak post–hoc tests. Error bars denote s.e.m.

Myelination and oligodendrocyte associated genes				
Gene		Fold change relative to +/+		
		+/+	MB+	MB-
Aspa	Aspartoacylase	-	1.3 ↑	-
Cldn11	Claudin 11	-	1.2 ↑	1.3 ↓
Clu	Clusterin	-	-	1.1 ↓
Cnp	2',3'-cyclic nucleotide 3' phosphodiesterase	-	1.2 ↑	1.1 ↓
Cst3	Cystatin C	-	1.1 ↑	1.1 ↓
Dpysl2	Dihydropyrimidinase-like 2	-	-	1.2 ↓
Ermn	Ermin, ERM-like protein	-	1.1 ↑	1.2 ↓
Fa2h	Fatty acid 2-hydroxylase	-	1.2 ↑	1.1 ↓
Gjc2	Gap junction protein, gamma 2	-	1.3 ↑	1.1 ↓
Gjc3	Gap junction protein, gamma 3	-	1.1 ↑	1.1 ↓
Gsn	Gelsolin	-	1.2 ↑	-
Gstm1	Glutathione S-transferase, mu 1	-	-	1.2 ↓
Hbb-b1	Hemoglobin, beta adult major chain	-	1.5 ↑	1.2 ↓
Lpar1	Lysophosphatidic acid receptor 1	-	1.1 ↑	1.2 ↓
Mag	Myelin-associated glycoprotein	-	1.2 ↑	1.1 ↓
Mal	Myelin and lymphocyte protein T cell differentiation protein	-	1.1 ↑	1.2 ↓
Mbp	Myelin basic protein	-	1.1 ↑	1.2 ↓
Mobp	Myelin-associated oligodendrocytic basic protein	-	1.1 ↑	1.3 ↓
Mog	Myelin oligodendrocyte glycoprotein	-	1.2 ↑	1.2 ↓
Ndrg1	N-myc downstream regulated gene 1	-	1.1 ↑	1.2 ↓
Nkx6-2	NK6 homeobox 2	-	1.2 ↑	1.1 ↓
Olig1	Oligodendrocyte transcription factor 1	-	1.1 ↑	1.1 ↓
Phgdh	3-phosphoglycerate dehydrogenase	-	1.1 ↑	1.1 ↓
Pllp	Plasma membrane proteolipid	-	1.2 ↑	-
Plp1	Proteolipid protein (myelin) 1	-	1.2 ↑	1.2 ↓
Prdx1	Peroxiredoxin 1	-	1.1 ↑	1.1 ↓
Tppp3	Tubulin polymerization-promoting protein family member 3	-	1.1 ↑	1.2 ↓
Tspan2	Tetraspanin 2	-	1.1 ↑	1.2 ↓
Tubb2b	Tubulin, beta 2B class IIB	-	1.1 ↑	1.1 ↓
Ugt8a	UDP galactosyltransferase 8A	-	1.2 ↑	1.2 ↓

Supplementary Table 2

Myelination and oligodendrocyte associated genes

CRISPR/Cas9 PAM sequences	
Name	**target site (spacer+PAM)**
gRNAf5_msTDP43_ptmutStart66End88	aggcagcgttg**c**agagc|agt**tgg**
gRNAf6_msTDP43_ptmutStart67End89	ggcagcgttg**c**agagca|gtt**ggg**
gRNAf7_msTDP43_ptmutStart68End90	gcagcgttg**c**agagcag|ttg**ggg**
single-stranded DNA (ssDNA) oligonucleotide	
ssDNA donor oligonucleotide_ TDP43msPtmut1 (mutation highlighted in red)	atgaactttggtgcttttagcattaacccagcgatgatggctg cggctcaggcagcgttgAagagcagttggggtatgatgggcat gttagccagccagcagaaccagtcgggcccatctg

Supplementary Table 3

CRISPR sequences

Preparation of DNA for genotyping

Extract DNA from ear biopsies at 10 days of age using QuickExtract (Epicentre).

Heat sample to 65°C for 15 minutes, briefly vortex and heat to 98°C for 2 minutes.

1µl was subsequently used for PCR.

Genotyping primers

Name	Sequence
Forward	TTGTTCAGCAGATTGCCACC
Reverse	CAGCAGTTCACTTTCACCCA

PCR cycling parameters

Temperature	Time
94°C	2 minutes
94°C	30 seconds
64°C	30 seconds
72°C	60 seconds
72°C	7 minutes

30x cycle PCR

Restriction digestion and gel electrophoresis

The Q331K mutation introduces a SapI/EarI restriction site, which facilitates genotyping

1) Column purify PCR products (Qiagen)
2) Digest with SapI at 37°C for 1 h
3) Resolve on a 1.5% agarose gel
4) A wild-type allele is indicated by a ~1 kb band. A mutant allele is indicated by a ~500 bp band (due to the overlap of two 500 bp digestion products)

Supplementary Table 4

Genotyping protocol

Primary antibodies for immunofluorescence			
Antigen (code)	**Antibody**	**Dilution**	**Source**
TDP-43 (ab41881)	Rabbit polyclonal	1:200	Abcam
Neurofilament heavy (ab4680)	Chicken polyclonal	1:200	Abcam
Parvalbumin (ab11427)	Rabbit polyclonal	1:200	Abcam
MAP2 (ab5392)	Chicken polyclonal	1:200	Abcam
Tau (A0024)	Rabbit polyclonal	1:500	Dako
NeuN (ab104224)	Mouse monoclonal	1:500	Abcam
AOX1 (PA5-36922)	Rabbit polyclonal	1:200	ThermoFisher Scientific
Synaptophysin (ab8049)	Mouse monoclonal	1:200	Abcam
βIII-tubulin (T2200)	Rabbit polyclonal	1:200	Sigma Aldrich
Secondary antibodies for immunofluorescence			
Antigen (code)	**Antibody**	**Dilution**	**Source**
Alexa fluor 488 (ab15007)	Goat anti-rabbit IgG	1:500	Abcam
Alexa fluor 568 (ab175471)	Goat anti-rabbit IgG	1:500	Abcam
Alexa fluor 488 (ab150113)	Goat anti-mouse IgG	1:500	Abcam
Alexa fluor 568 (ab175473)	Goat anti-mouse IgG	1:500	Abcam
Alexa fluor 568 (ab175477)	Goat anti-chicken IgY	1:500	Abcam
Primary antibodies for western blotting			
Antigen (code)	**Antibody**	**Dilution**	**Source**
TDP-43 (ab41881)	Rabbit polyclonal	1:1000	Abcam
Cyclophilin (ab41684)	Rabbit polyclonal	1:1000	Abcam
Nucleoporin (mab414)	Mouse monoclonal	1:500	Abcam

Supplementary Table 5

Primary antibodies used for immunofluorescence and immunoblotting

Gene	Forward	Reverse
Tardbp Intron 7 exclusion	TTCATCTCATTTCAAATGTTTATGGAAG	ATTAACTGCTATGAATTCTTTGCATTCAG
Sort1 Exon 17b inclusion	AACCCCACAAAGCAGGACT	CTGCTACGACTGTGACAAGC
Sort1 Exon 17b excluded	ATCCCAGGAGACAAATGCCA	TGGAATTCTGCTTTGTGGGG
0N *Mapt*	TTAAAAGCCGAAGAAGCAGGC	CTGGAGGAGTCTTAGGGCTG
1N *Mapt*	CGCCAGGAGTTTGACACAAT	CCTGCTTCTTCGGCTTCAG
2N *Mapt*	CATGGCTTAAAAGAGTCTCCCC	CCTGCTTCTTCGGCTGTAAT
Mbp (Basic)	GCCCTCTGCCCTCTCATG	TCTTGAAGAAATGGACTACTGGG
Mbp (Golli)	ATTGGGTCGCCATGGGAAA	CGCTTCTCTTCTTTCCAGCC
Matr3	GCACTTTGGTTTCAGGGGAG	CTGTTAGGAATCCGCAGCAC
Matr3 (Exon 14)	AGCAGCCTTCCTCATTATCAGA	TTCCTTCTTCTGCCTCCGTT
Sqstm1	CCAGTGATGAGGAGCTGACA	CCGGCACTCCTTCTTCTCTT
Sqstm1 (TDP-43 ^{Q331K} variant)	ACCCATCTACAGGCTGATCC	GTCTGTAGGAGCCTGGTGAG

Supplementary Table 6

Primers for quantitative PCR